Estimation and Correction of Rotation Induced Artifacts using Autocorrection and A Linear Distortion Model

Kiaran P. McGee[1], Joel P. Felmlee[1], Clifford R. Jack Jr.[1], Armando Manduca[1], Richard L. Ehman[1]
[1]Mayo Clinic, MR Research Lab, Rochester, MN USA;

Introduction

Autocorrection is a new retrospective adaptive motion correction algorithm for reducing motion-induced image artifacts[1]. It requires no apriori knowledge of the motion history. Instead, an iterative approach is used to 'guess' the motion record that produces the greatest reduction in image artifacts, as measured by an image metric. Most recently, autocorrection has been shown to reduce rotation-induced artifacts in high resolution in three-dimensional time-of-flight (3D ToF) MR angiography (MRA) exams of the circle of Willis[2] by applying a linear motion model and correcting small regions distal from the center of rotation. However, this model is limited to correcting small sub regions of an image, and provides an estimate of linear motion rather than the record of rotation. The purpose of this paper is to report on the application autocorrection to estimate the view-to-view rotation record in 3D ToF MR angiograms which can then be used to generate a global distortion correction map.

Methods

Consider the simple case of a single object rotating from point A to B about a fixed point(Fig. 1). The rotation angle, α, can be estimated using the arc tan relationship ($\alpha = \tan^{-1}[\Delta y_2 - \Delta y_1/\Delta x]$).

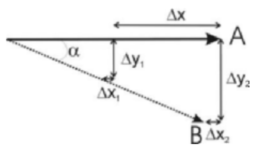

Figure 1: Rotation of an object from point A to point B.

This concept is extended to MR imaging by performing autocorrection over two separate, non-contiguous regions. The displacement records, $\Delta y_1(i)$ and $\Delta y_2(i)$ from these two regions are used to calculate the record of rotation during imaging ($\alpha(i) = \tan^{-1}[\Delta y_2(i) - \Delta y_1(i)/\Delta x]$), where i is the view number index). Knowledge of α(i) allows calculation of a view-to-view displacement map as a function of x using the equation for a straight line ($y = mx + b$). The slope is given by tan α(i) and the intercept is calculated by substitution of $\Delta y_1(i)$ or $\Delta y_2(i)$, tan α(i), and solving for b. Conversion of this displacement record to a phase correction map allows for a global correction of rotation induced artifacts along the y axis.

Results

Figure 2(A) shows a maximum intensity projection (MIP) image generated from a simple phantom designed to mimic cerebral vessels. In this instance the phase encoding direction was along the ordinate. The two regions of interest represent the regions over which autocorrection was performed, allowing calculation of the two view-to-view displacement records, $\Delta y_1(i)$ and $\Delta y_2(i)$. The geometric relationship established to calculate the view-to-view rotation angle, α(i), and the displacement map, Δy(x,i) is also shown in (A). Figure 2(B) is the calculated rotation record and 2(C) shows the MIP image after application of the two-dimensional phase map. In the reconstructed image, artifacts remain in the image. This is due to the fact that the motion along the abscissa have not been corrected. These can be corrected by performing autocorrection again using two regions of interest orthogonal to the first pair so that the histories $\Delta x_1(i)$ and $\Delta x_2(i)$ are determined but at the expense of increased computation.

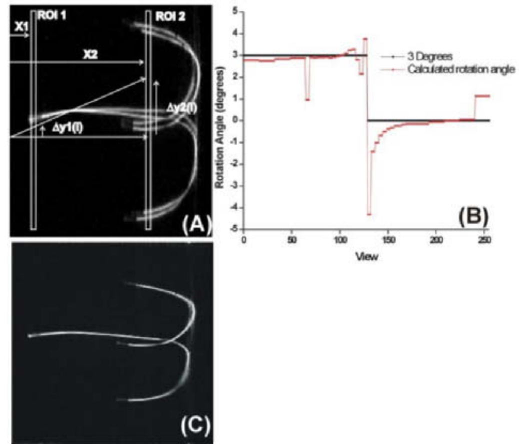

Figure 2: Application of distortion model to angiographic phantom image. (A) original MIP image with motion corruption and ROIs (B) Calculated and actual rotation angles. (C) Mip image after distortion correction.

Figure 3(A) shows a MIP generated from a 3D ToF gradient recalled echo sequence (TE 6.9, TR 43 ms, 25 degree flip angle, 18 cm field of view, 244/32 phase encodings (ky/kz) and 2.5 mm slice thickness) volunteer exam corrupted by rotation in the axial plane after acquisition of ½ the k-space views. (B) shows the MIP image after autocorrection over a single region of interest located over the anterior cerebral arteries. Note the degradation of objects outside the correction region (arrow). Autocorrection was performed over a second region that included the posterior cerebral arteries. For the two regions, autocorrection generated displacement histories $\Delta x_1(i)$ and $\Delta x_2(i)$. The phase correction map derived from these values was then applied to the entire 3D k-space data set, resulting in the autocorrected MIP image shown in 3(C). In this final image, all regions of the MIP appear free from motion artifacts.

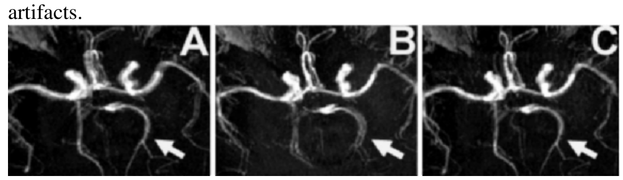

Figure 3: MIP images generated from a motion corrupted 3D ToF MRA of a normal volunteer. (A)Motion corrupted image. (B) MIP image after autocorrection of small ROI located over anterior cerebral arteries. (C) MIP image generated from linear distortion.

Discussion

Clinical implementation of autocorrection for complex motion histories in large MR data sets is limited by the huge computational requirements. Using the approach presented, it is possible to firstly calculate and then correct for rotation induced artifacts using a simple linear model which is inherently quicker than true rotation autocorrection algorithms. This rotation estimate can also be used as an optimized starting point for a true rotation autocorrection algorithm.

References

1. Manduca A, et al. Radiology 1999;215:904-909.
2. McGee KP, et al. AJR In Press.